

**LNF-96/050**

## **Performance of F101 Radiation Resistant Lead Glass Shower Counters**

H. Avakian, N. Bianchi, G.P. Capitani, E. De Sanctis, A. Fantoni,  
V. Giourdjian, R. Mozzetti, V. Muccifora, M. Nupieri, A.R. Reolon, P. Rossi,  
J.F.J. van den Brand, M. Doets, T. Henkes, M. Kolstein, A. Airapetian,  
N. Akopov, M. Amarian, R. Avakian, A. Avetissian, V. Garibian, S. Taroian,  
P. Galumian, A. Simon, B. Bray, B. Filippone, A. Lung

*Nuclear Instruments & Methods A, 378, 155-161, (1996)*



ELSEVIER

# Performance of F101 radiation resistant lead glass shower counters

H. Avakian<sup>a</sup>, N. Bianchi<sup>a</sup>, G.P. Capitani<sup>a</sup>, E. De Sanctis<sup>a</sup>, A. Fantoni<sup>a</sup>, V. Giourdjian<sup>a</sup>,  
R. Mozzetti<sup>a</sup>, V. Muccifora<sup>a</sup>, M. Nupieri<sup>a</sup>, A.R. Reolon<sup>a</sup>, P. Rossi<sup>a</sup>, J.F.J. van den Brand<sup>b,c</sup>,  
M. Doets<sup>b</sup>, T. Henkes<sup>b</sup>, M. Kolstein<sup>b</sup>, A. Airapetian<sup>d</sup>, N. Akopov<sup>d</sup>, M. Amarian<sup>d</sup>,  
R. Avakian<sup>d</sup>, A. Avetissian<sup>d</sup>, V. Garibian<sup>d</sup>, S. Taroian<sup>d</sup>, P. Galumian<sup>e</sup>, A. Simon<sup>f</sup>, B. Bray<sup>g</sup>,  
B. Filippone<sup>g</sup>, A. Lung<sup>g</sup>

<sup>a</sup>Laboratori Nazionali di Frascati dell'INFN, C.P. 13, Via E. Fermi 40, I-00044 Frascati (Roma), Italy

<sup>b</sup>NIKHEF, Kruislaan 411, 1098 SJ Amsterdam, The Netherlands

<sup>c</sup>Vrije Universiteit Amsterdam, Rm. T-269, de Boelelaan 1081, 1081 HV Amsterdam, Netherlands

<sup>d</sup>Yerevan Physics Institute, Alikhanian Brothers St. 2, Yerevan AM-375036, Armenia

<sup>e</sup>Univ. de Lausanne, Inst. de Phys. Nucléaire, B.S.P. Dorigny, CH-1015 Lausanne, Switzerland

<sup>f</sup>New Mexico State University, Box 3D-Gardiner Hall, Las Cruces, NM 88003-0001, USA

<sup>g</sup>California Institute of Technology, 106-38, Pasadena, CA 91125, USA

Received 9 April 1996

## Abstract

The performance of F101 lead glass as a Cherenkov radiation material was studied. A  $3 \times 3$  array of  $9 \times 9$  cm<sup>2</sup> and 50 cm length counters showed an energy resolution of  $\approx 5.0\% / \sqrt{E(\text{GeV})}$ , good linearity in the energy range from 1 to 25 GeV and  $\pi^-/e$  rejection of  $\approx 4 \times 10^{-4}$ .

## 1. Introduction

The HERMES experiment [1], designed for a precise study of the spin structure of the nucleon [2], will measure spin-dependent effects in deep inelastic scattering of electrons from the proton and neutron using the longitudinally polarized electron beam of the HERA storage ring [3] and polarized internal gas targets of hydrogen, deuterium and <sup>3</sup>He [4].

The angle and the energy of the scattered electrons are determined by track reconstruction from drift chambers in front and behind a spectrometer magnet and proportional chambers in the magnet. The yield of background particles emitted from the target is mainly suppressed at the trigger level by a calorimeter in conjunction with a scintillator hodoscope.

The HERMES calorimeter is designed to provide the following functions:

- first level trigger on scattered electrons, with suppression of the low energy background in conjunction with an active preshower (hodoscope),
- rejection of high energy pions by a factor of  $\geq 10$  at a first level trigger and  $\geq 100$  in the off-line analysis in the energy range of 4–10 GeV,
- reasonably good energy resolution for scattered electrons,

– uniformity of response relative to impact point and angle of incidence,

– coarse position measurement for scattered electrons.

Moreover, it must have high radiation hardness to provide long term stability of response in the HERA environment.

The solution chosen to meet these requirements consists of 840 radiation resistant F101 lead glass blocks arranged in a two wall configuration (one wall above and the other below the beam) with PMT viewing from the rear, as shown in Fig. 1. Each wall is composed of 420 identical lead-glass blocks, which have an area  $9 \times 9$  cm<sup>2</sup> and a length of 50 cm (about  $18 X_0$ ) and is stacked in a  $42 \times 10$  array.

This paper presents the results of a study of F101 block characteristics done on test beams at CERN and DESY.

## 2. F101 lead-glass counters

The lead-glass (LG) used was F101, made by Lytcarino [5], whose properties are listed in Table 1. Each block was mirror polished, wrapped in 2 mils thick aluminized mylar foil and covered with a 5 mils thick Tedlar foil to provide light isolation.

The cathode window of the 3" photo-multiplier Philips

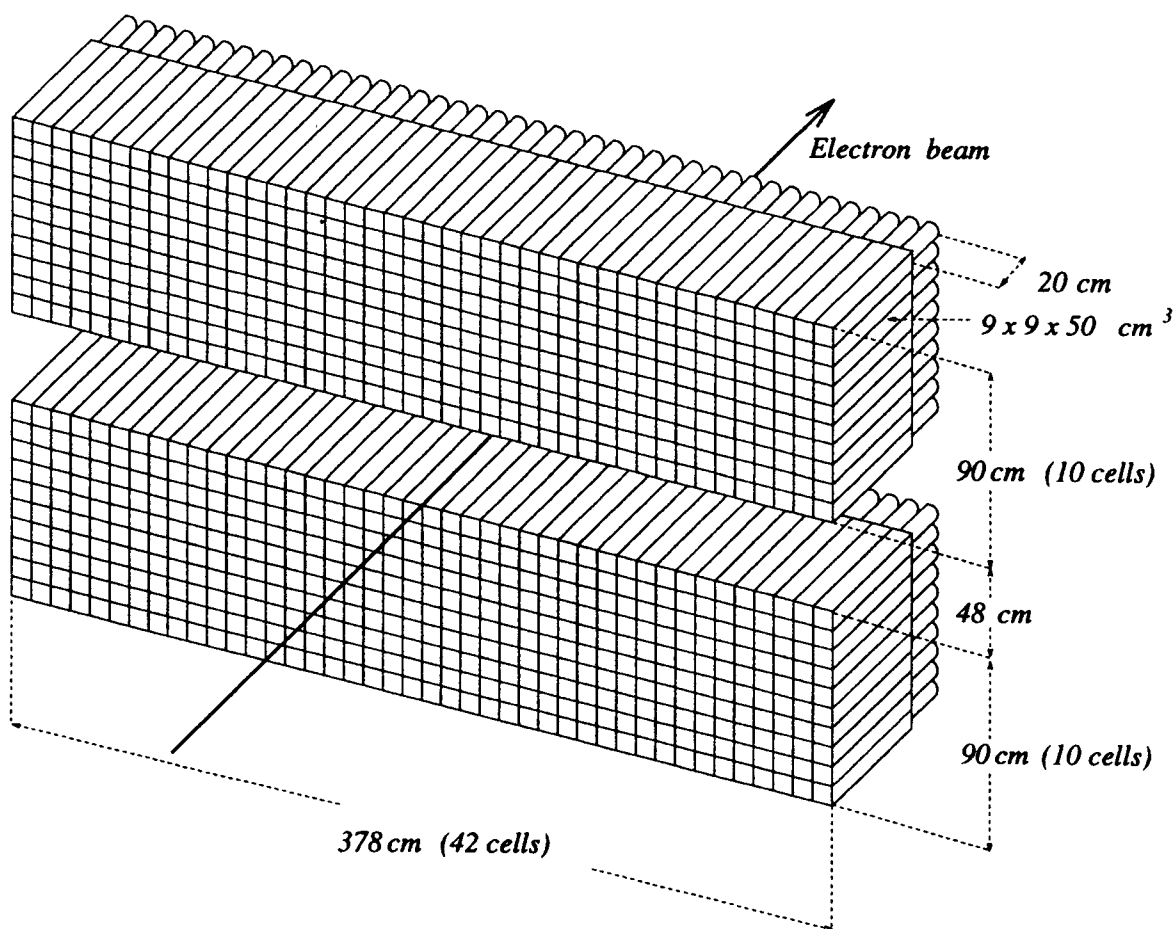


Fig. 1. Isometric view of the HERMES calorimeter.

XP3461 (PMT) were glued to the lead glass with a silicon glue (SILGARD 184) with refraction index 1.41. A  $\mu$ -metal magnetic shield surrounded the PMT. A surrounding aluminium tube that is housing the  $\mu$ -metal and providing light-tightness is fixed to a flange, which is glued to the surface of the lead glass. This flange is made of titanium matching the thermal expansion coefficient of F101 LG.

Measurements of the radiation hardness of F101 LG blocks for  $\gamma$  rays [6] and for high energy hadrons [7] have shown that an accumulated dose of 2000 rad produces a degradation of transmittance less than 1%. Thus the F101

LG is 10–50 times less sensitive to radiation damage than SF2 lead-glass [8], depending on dose and light wavelength. This is due to the contribution of cerium which as a drawback worsens the optical transmission characteristics.

Fig. 2 shows the light transmittance from a 8.9 cm thick F101 LG block.

The blocks were produced at the factory by groups (mouldings) with identical optical features, but having different absorption coefficients from moulding to moulding. Blocks from different mouldings showed light transmittance curves that lie within the two curves in Fig. 2. As the working wavelengths of light exceed 500 nm, the spectral distribution well matches the spectral response of multi-alkali or green extended photo-tubes.

All physical and optical characteristics of F101 LG, the quantum efficiency of the Philips XP3461 PMT and the refraction indices of its window and glue were used to provide a realistic simulation of the detector. In Fig. 3 is shown the response (provided by a simulation based on GEANT code [9]) of the F101 LG blocks to different incident particles of same momenta  $p$  as a function of  $E/p$ ,  $E$  being the energy deposited in the lead glass. The electrons which leave all their energy producing a shower in the lead glass appear as a peak near 1; pions, which usually leave only a fraction of their energy in the lead

Table 1  
Chemical composition and physical properties of the F101 LG

Chemical composition [weight%]	
Pb <sub>3</sub> O <sub>4</sub>	51.23
SiO <sub>2</sub>	41.53
K <sub>2</sub> O	7.0
Ce	0.2
Radiation length [cm]	2.78
Density [g/cm <sup>3</sup> ]	3.86
Critical energy [MeV]	17.97
Molière radius [cm]	3.28
Refraction index	1.65
Thermal expansion coefficient [C <sup>-1</sup> ]	$8.5 \times 10^{-6}$

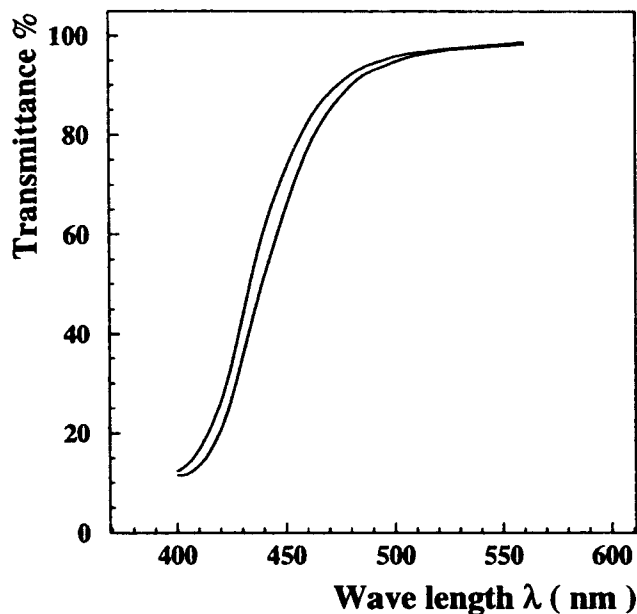


Fig. 2. Transmittance for 8.9 cm thick F101 LG blocks.

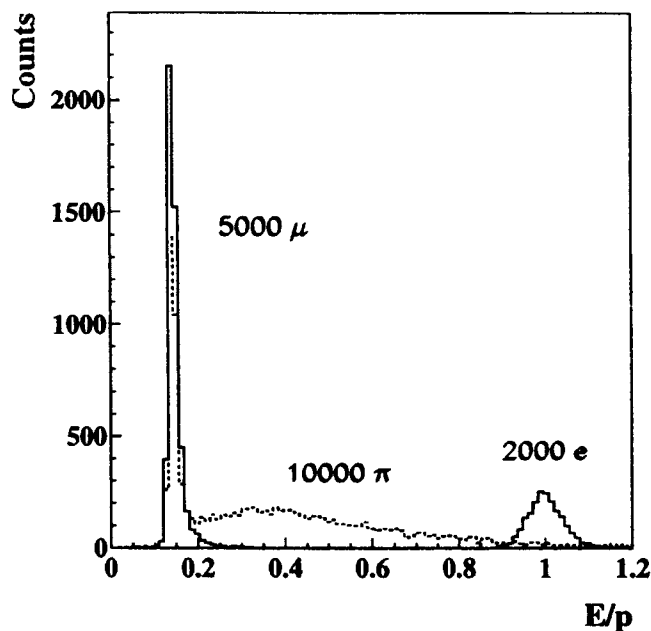


Fig. 3. Distribution of the ratio of the energy deposited  $E$  and momentum  $p$  for  $e$ ,  $\pi$  and  $\mu$  of 5 GeV/ $c$  momentum.

glass, have a long tail due to hadronic showers, while muons undergo mainly ionization losses and are good for defining the minimum ionizing particle value.

### 3. Measurements with test beams

The performance of the F101 LG was studied exposing several counters to the electron and pion test beams at CERN (PS T9, SPS X3 and SPS X1 beams) [10] and to the electron test beam 21 at DESY II; the characteristics of these beams are given in Table 2.

#### 3.1. Choice of detector configuration

The energy resolution and the  $\pi^-/e$  separation have been measured for arrays of  $3 \times 3$  F101 blocks having the same cross section ( $9 \times 9 \text{ cm}^2$ ) and different lengths (30, 40 and 50 cm, respectively) both with and without a  $2X_0$  thick preshower (1 cm of lead + 1 cm of plastic scintillator) in front of the lead-glass array.

The longer blocks showed a better resolution, but a higher light attenuation. This attenuation produces a reduction of the light yield from electron-initiated showers with respect to the ones from hadron showers, because hadrons lose energy more uniformly along their path through the LG block. For a single F101 LG block of 30 cm length it was found a  $2 \times 10^{-3}$  rejection factor in the energy interval from 4 to 8 GeV for a 95% electron detection efficiency: this is more than 5 times better than for the 50 cm length. However, as pointed out previously by Appel et al. [11], hadron rejection is remarkably improved by the addition of a preshower detector, which provides information on the longitudinal development of the electromagnetic shower. Demanding that a large energy be deposited in the preshower enhances the probability that the shower is originated by electrons. Moreover, the preshower provides a bias against such processes, as the charge exchange  $\pi^- + p \rightarrow \pi^0 + n$ , where most of the energy of charged pions goes to neutral pions. These neutral pions immediately decay into  $\gamma$ -rays starting a cascade which is indistinguishable from an electron-initiated shower.

Table 2  
Test beam parameters

Lab	CERN	CERN	CERN	DESY
Test beam	PS T9	SPS X3	SPS X1	N 21
Particle	$e$	$e$	$e$	$e$
	$\pi$		$\pi$	
Intensity [ $\text{s}^{-1}$ ]	$10^5 - 10^4$	$10^3 - 10^4$	$10^3 - 10^2$	10
	$10^5 - 10^4$		$10^4 - 10^2$	
$\Delta p/p$	$\pm 1.1\%$	$\pm 1\%$	$\pm 0.3\%$	$\pm 4\%$
$P_{\text{max}}$ [GeV]	10	50	80	6
Purity	$\leq 10^{-4}$	–	$10^{-3}$	

The preshower allows the first radiation lengths to be of lead, which has a smaller number of interaction lengths per radiation length than does the lead glass, and that the shower be examined after a small number of radiation lengths. The overall detection efficiencies of the calorimeter and preshower for electron and pion response are plotted in Fig. 4. Putting the cuts at the minimum of the ratio between pion and electron efficiencies in the lead glass ( $\approx 95\%$ ) and at the value  $\approx 98\%$  in the preshower yields a hadron rejection of  $\approx (4 \pm 2) \times 10^{-4}$ .

In conclusion: in these test measurements, the 50 cm thickness matrix with a two radiation length thick preshower detector gave the best results. Thus unless differently stated all measurements described below were performed with the counter array of 50 cm thickness with preshower.

A very good agreement was also found between the simulation and the data (see as an example Figs. 7 and 9)

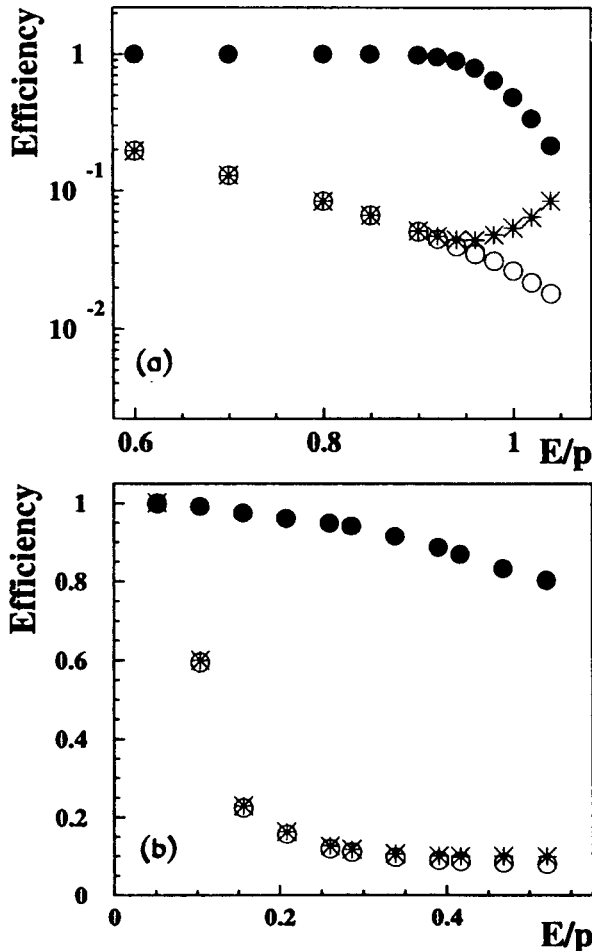


Fig. 4. Efficiency for electron and pion detection (a) in lead glass and (b) in preshower as a function of a cut on the ratio of deposited energy to the mean. Solid circles: electron efficiency; open circles: pion efficiency; asterisks: pion to electron efficiency ratio.

and this provided a reliable way to interpolate and/or extrapolate the experimental results.

### 3.2. Linearity of the response

The absolute energy calibration measured for a  $3 \times 3$  matrix lead-glass counters, is shown in Fig. 5. As seen in the top figure the linearity is very good: all the data, apart from the one at 1 GeV, are reproduced better than 1% by the linear fit  $E = 0.32 + 0.40 \times 10^{-2} \text{ ADC}$ , as shown in the bottom part of the figure, where the ratio between the fit and the data is given. However, for low energies the data are better described by the cubic dependence  $E = 0.19 + 0.43 \times 10^{-2} \times \text{ADC} - 0.10 \times 10^{-6} \times \text{ADC}^2 + 0.10 \times 10^{-10} \times \text{ADC}^3$  (Fig. 5 bottom also shows the ratio between this cubic fit and the data) due to the presence of the

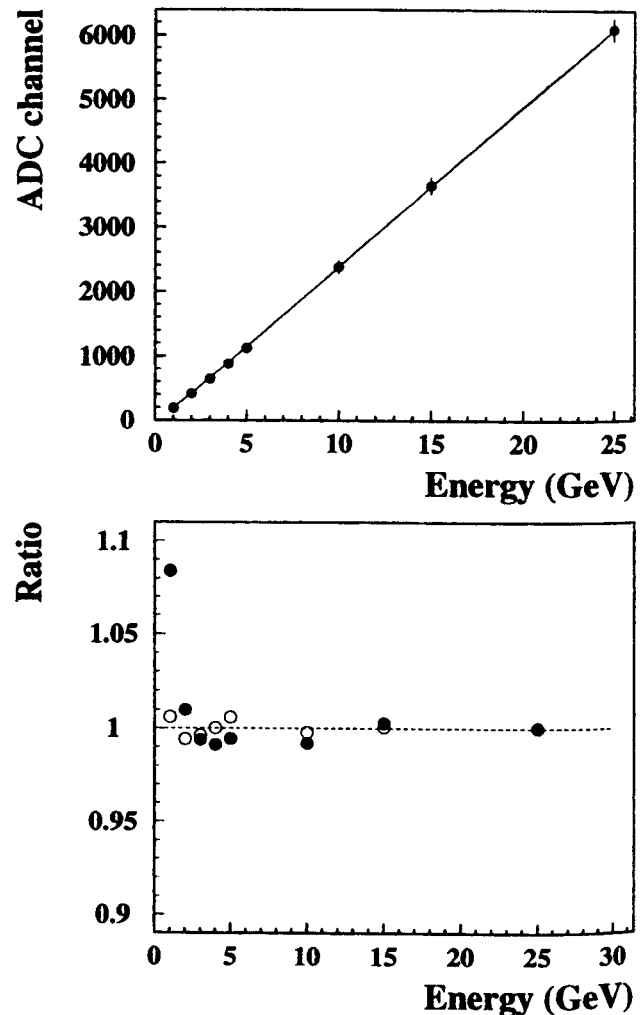


Fig. 5. Top: Linearity of the LG block response versus the incident energy (the solid line is a linear fit to the data). Bottom: The ratios between the linear fit and the data (full circles) and cubic fit and the data (empty circles). The dashed line at ratio = 1 is a guide for the eye.

lead preshower before the calorimeter and to the strong attenuation of light in the block.

### 3.3. Spatial and angular dependence of the response

A particle entering a counter produces light also in the adjacent counters of the array, the energy sharing depending on the lateral spread of the shower and on the impact point and angle of incidence. Then, in order to measure accurately the energies of electromagnetic particles, the position dependence of the response of the lead-glass array should be taken into account.

Fig. 6 shows the position dependence at 3 GeV of the pulse height in two neighbouring counters as a function of the impact point. The electron beam hit the front surface of the lead-glass counters at a right angle. As shown the sum of the pulse heights obtained by the two adjacent counters is constant within 2%. Moreover, it was found that for incident angles within the acceptance of the detector, 2°–9°, the variation of the response is less than 1% for the central block in the array.

Then from the measurements of the energy deposited in adjacent blocks when electrons enter the block near an edge it is possible to estimate the mean lateral shower extension. The leakage of the shower into neighbouring modules can be exploited to determine the impact point of the incoming photons, with higher precision than expected from the lateral dimensions of the modules.

Fig. 7 gives the fractional energy leakage from a block

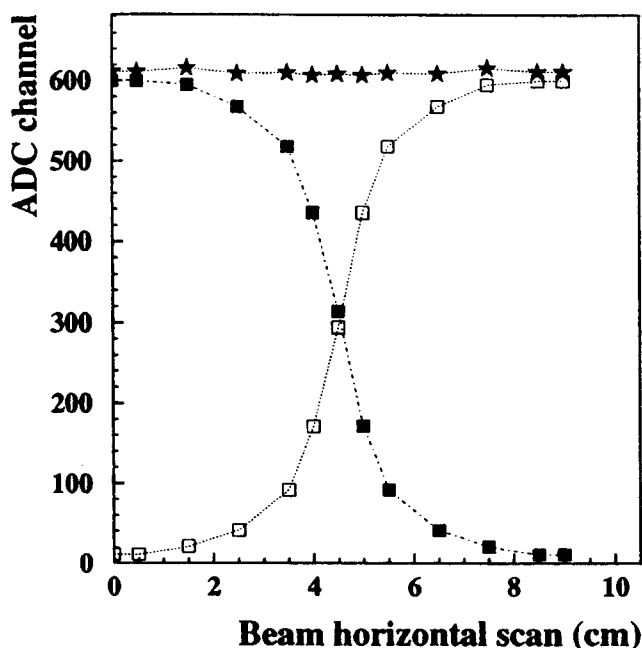


Fig. 6. Energy deposition in adjacent blocks. The positions 0 cm and 9 cm correspond to the centers of the left and right blocks respectively. Solid squares: left block; open squares: right block; stars: sum of two blocks.

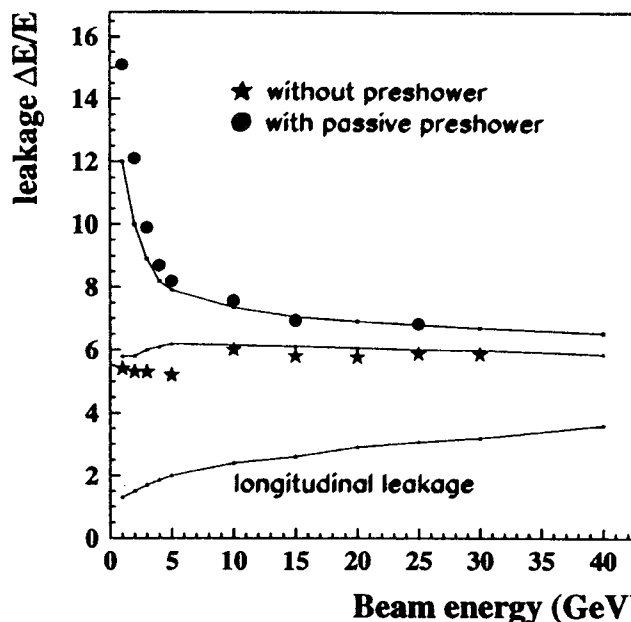


Fig. 7. Energy leakage (in percent) from the central block of a 3 × 3 matrix for central impact and normal incidence of the electrons. The stars are data without preshower, circles with passive preshower, and the solid curves are results from simulations.

for electrons incident perpendicular to the surface of the counter with and without the preshower. The data are compared to the leakage values provided by GEANT simulations (solid line curves). The longitudinal leakage predicted by the simulation is also given. As expected, this leakage increases with increasing incident electron energy. At the same time the center shower development shifts longitudinally to the center of the block thus decreasing the mean path of Cherenkov photons to the PMT and the losses due to attenuation of light in the LG block. Due to this the linearity of the response is quite good also for high energies, where the longitudinal leakage is higher.

### 3.4. The energy resolution

In Fig. 8 is shown the measured energy resolution of electrons as a function of the incident electron energy in the range 1–30 GeV. The open circles are the values of the energy resolution obtained by fitting the electron pulse height distributions with a Gaussian function whose parameters were adjusted to minimize chi-squared. The solid circles are the values obtained after the “compensation” for the energy deposited in the preshower which, as said above, produces a non linearity of the response at low energy. The clear correlation observed between the energy deposition in the preshower and calorimeter was used to make this correction.

The compensation constant was derived by fitting the compensated response of LG blocks with preshower to the

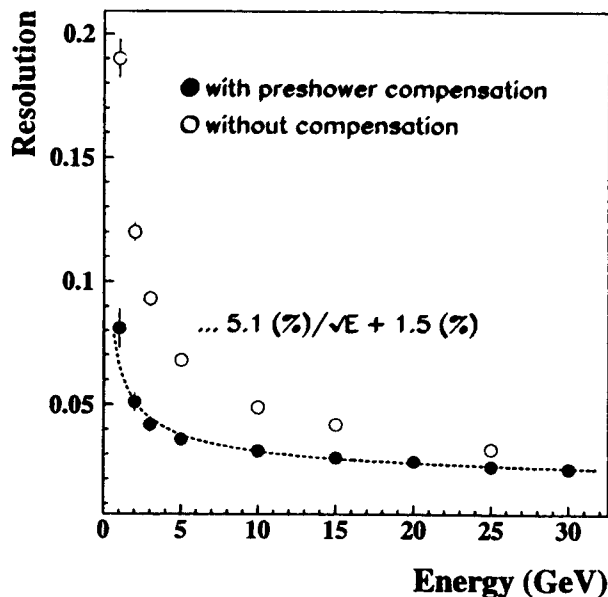


Fig. 8. Energy resolution of calorimeter  $\sigma(E)/E$  versus the energy: solid and open circles are data without and with compensation for the energy deposited in the preshower. The error bars take into account the statistical accuracy and the beam resolution. The latter gives a big contribution at low energy, as shown in Table 2. The line shows the parameterization described in the text.

response of blocks without the preshower. As seen, the procedure of “compensation” significantly improves the energy resolution of the electron signal.

The dotted curve is a fit of the data to the form  $\sigma(E)/E$  [%] =  $A/\sqrt{E}$  [GeV] +  $B$ . The obtained values for  $A$  and  $B$  are  $(5.1 \pm 1.1)$  and  $(1.5 \pm 0.5)$  respectively, similar to the resolutions obtained for other large lead glass calorimeters [12–17].

### 3.5. Pion–electron identification

As stated above an important function of HERMES calorimeter is the identification of electrons amid a large flux of hadrons. The ratio of pions from target to electrons within the spectrometer acceptance is expected to be about 400 for 4.5 GeV particles.

In Fig. 9 is shown the combined pion rejection factor of the calorimeter for the preshower arrangement measured for a 50 cm length single block for a 95% electron detection efficiency. As seen the rejection with the preshower is  $\approx (4 \pm 2) \times 10^{-4}$ . Moreover, the influence on the pion electron rejection of the refraction index of the glue between the lead glass and PMT was investigated analysing the angular and spatial distributions of Cherenkov photons. It was found that the glue with refraction index 1.41 gives better rejection than the one with refraction index 1.59 which is equal to the one of the PMT window. This is because the glue is working as a filter cutting the

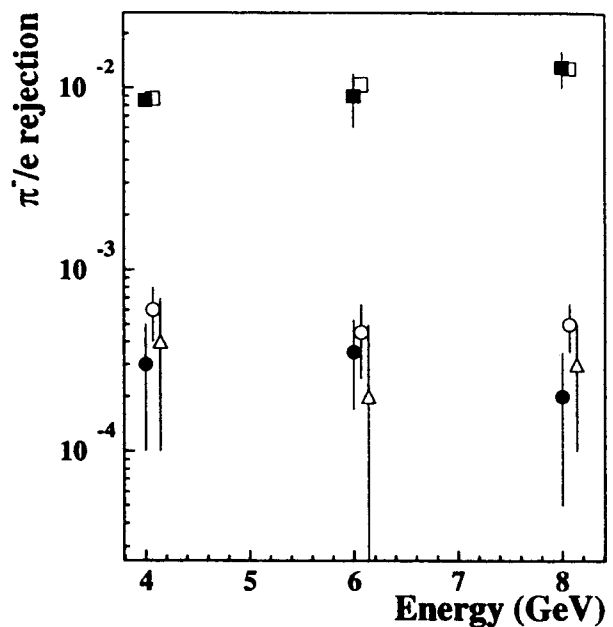


Fig. 9. Pion/electron rejection in a single block of the calorimeter and preshower corresponding to an electron efficiency of 95%. Filled and empty points are experimental results and simulation respectively. Squares refer to the case of calorimeter only and circles to the case of calorimeter and preshower; triangles refer to the reduced cluster, as described in the text. The simulation results are plotted at energy values slightly shifted, to make them more visible.

Cherenkov photons arriving at the PMT window with larger angles.

It was also found that the  $\pi^-/e$  rejection can be further improved by a factor of two by considering only a reduced cluster (see Fig. 9): specifically the one formed by blocks at a distance less than  $d/2$  from the initial particle track (where  $d$  is the size of the cell) instead of a  $3 \times 3$  matrix cluster. This lateral cut reduced significantly the yield of pions, which produce showers with wider spatial distribution than the electrons.

## 4. Conclusions

The performance of F101 lead glass as a radiating material for the electromagnetic calorimeter of the HERMES experiment has been measured. A  $3 \times 3$  array of  $9 \times 9$  cm<sup>2</sup> area and 50 cm length counters showed:

(i) an energy response to electrons linear within 1%, over the energy range 1–30 GeV;

(ii) an energy resolution  $\sigma/E$  [%] =  $(5.1 \pm 1.1)/\sqrt{E}$  [GeV] +  $(1.5 \pm 0.5)$ ;

(iii) a  $\pi^-/e$  rejection of  $\approx (4 \pm 2) \times 10^{-4}$ , in combination with a preshower consisting of 1 cm thick lead and 1 cm thick scintillator. The rejection can further be improved by a factor of 2 taking into account the lateral distribution of the shower.

## Acknowledgements

We thank G. Baldacchini (ENEA-CRE Frascati) for providing the detector for the F101 light transmission measurements, the NMSU-HERMES group for providing the splitters and delay modules of the electronics, W. Brückner for providing the data acquisition system and the Frascati HERMES technical staff (M. Albicocco, A. Orlandi, W. Pesci, A. Viticchié) for the continual and effective assistance during the work.

This work was supported in part by “Stichting voor Fundamenteel Onderzoek de Materie” (FOM), which is financially supported by the “Nederlandse Organisatie voor Wetenschappelijk Onderzoek” (NMO).

## References

- [1] HERMES Collaboration, Proposal DESY-PRC 90/01 (1990).
- [2] M. Düren, K. Rith, Proc. of Physics at HERA, vol. 1 DESY Oct. 91, p. 427.
- [3] D.P. Barber et al., Phys. Lett. B 343 (1995) 436.
- [4] HERMES collaboration, Technical Design Report DESY-PRC 93/06 (1993).
- [5] Lytcarino factory of optical glasses, 140061 Lytcarino Moscow, Russia.
- [6] M. Kobayashi et al., KEK internal report 93-178 (1993).
- [7] A.V. Inyakin et al., Nucl. Instr. and Meth. 215 (1983) 103.
- [8] M. Holder et al., Nucl. Instr. and Meth. 108 (1973) 541.
- [9] R. Brun et al., CERN DD/EE/84-1 (1986).
- [10] Experiment at CERN in 1992 Geneva, November 1992.
- [11] J. Appel et al., Nucl. Instr. and Meth. 127 (1975) 495.
- [12] K. Ogawa et al., Nucl. Instr. and Meth. A243 (1986) 58; T. Sumiyoshi et al., Nucl. Instr. and Meth. A271 (1988) 432.
- [13] H. Stroher et al., Nucl. Instr. and Meth. A269 (1988) 568.
- [14] G.T. Bartha et al., Nucl. Instr. and Meth. A275 (1989) 59.
- [15] H. Baumeister et al., Nucl. Instr. and Meth. A292 (1990) 81.
- [16] L. Bartoszek et al., Nucl. Instr. and Meth. A301 (1991) 47.
- [17] W. Brückner et al., Nucl. Instr. and Meth. A313 (1992) 345.